On the electronic structure and stability of icosahedral r-$X_2Z_{10}H_{12}$ and $Z_{12}H_{12}^{2-}$ clusters; r = {*ortho*, *meta*, *para*}, X = {C, Si}, Z = {B, Al}†‡

Josep M. Oliva,[a] Paul von Ragué Schleyer,[b] Gabriel Aullón,[c] José I. Burgos,[d] Antonio Fernández-Barbero[e] and Ibon Alkorta[f]

Received 18th November 2009, Accepted 23rd February 2010
First published as an Advance Article on the web 26th March 2010
DOI: 10.1039/b924322d

We report on the electronic structure of the 12-vertex icosahedral clusters r-$X_2Z_{10}H_{12}$ and $Z_{12}H_{12}^{2-}$, where X = {C, Si} and Z = {B, Al}. The least stable cluster—with the lowest HOMO–LUMO gap (E_g)—corresponds to the *ortho*-$X_2Z_{10}H_{12}$ isomers for all values of X = {C, Si} and Z = {B, Al}. The well-known energetic order E(*para*) < E(*meta*) < E(*ortho*) for r-carboranes is also valid for all compounds except r-$C_2Al_{10}H_{12}$. Substitution of two atoms of carbon or silicon into the icosahedral cage $B_{12}H_{12}^{2-}$ enhances considerably the stability of the system as analyzed from E_g gaps, as opposite to $Al_{12}H_{12}^{2-}$, where similar gaps are found upon double carbon or silicon substitution regardless of the positions in the cage. In order to highlight similarities and differences in the title clusters, topological analysis of the electron density was performed, together with analysis of the deviation from polyhedron icosahedral form with (*i*) volumes, skewness and kurtosis calculations; and (*ii*) continuous shape measures.

1. Introduction

The icosahedral $B_{12}H_{12}^{2-}$ borane and r-$C_2B_{10}H_{12}$ carboranes (r = *ortho*, *meta*, *para*) are very stable and well known compounds with a wide range of direct and potential applications such as in nanoscience,[1,2] medicine,[2,3] ionic liquids,[2] metal-ion extraction,[4,5] nuclear fusion,[5,7] non-linear optics,[8] homogeneous catalysis,[9] liquid crystals,[10] and plasmonics.[11]

The synthetic efforts towards combinations of the above (car)borane cages have led in the last four decades to an explosion of a rich variety of structures combined with organic groups,[12,13] transition-metal atoms[14] and the cages themselves to combine into carborod or rigid-rod finite 1D polycarboranes (oligo-r-carboranes),[15,16] whilst supercluster systems based on icosahedral carborane clusters,[17] and molecular self-assemblies with a carborane backbone have also been achieved.[1]

From now on, unless otherwise stated, the notation *ortho*, *meta* and *para* for any r-$X_2Z_{10}H_{12}$ isomer will be shortened to *o*-, *m*- and *p*- respectively. While $B_{12}H_{12}^{2-}$ and r-carborane chemistries are well-known and founded, little is known regarding analogous structures from the viewpoint of the periodic table if we take into account the same number of valence electrons: hence, we may ask what stability and reactivity one should expect when substituting C ↔ Si and B ↔ Al in the above clusters, leading to the species $Al_{12}H_{12}^{2-}$, r-$Si_2B_{10}H_{12}$, r-$C_2Al_{10}H_{12}$ and r-$Si_2Al_{10}H_{12}$. With regards to the 12-vertex icosahedral silaboranes, r-$Si_2B_{10}H_{12}$ analogues are much more reactive as compared to r-carboranes and only compounds with substituents in positions 1 and 2 from *ortho*-$Si_2B_{10}H_{12}$ or 1,2-$Si_2B_{10}H_{12}$[18–20] are known so far to our knowledge. We are not aware of published material on 12-vertex carbaluminium or silaluminium compounds with icosahedral r-$X_2Al_{10}H_{12}$ formulae, X = {C, Si}; only crystal structures including the Al_{12} icosahedral cluster have been published.[21–24] Icosahedral $Al_{13}I^-$ and the "closed-shell" magic cluster Al_{13}^- with an endohedral Al atom in the center—both defined as "superhalogens"—have been detected.[25]

In the last ten years, we have been interested in how the electronic structure of the (car)borane cages—and connections among them in different dimensions—changes as a function of substituent, charge, spin and wave function nature (excited state, ground state, *etc*),[26] predicting also an ejection mechanism for the detection of yet-unknown endohedral (car)boranes:[27] following this research line, we extend it now to the comparison of the relative stabilities of r-$X_2Z_{10}H_{12}$ and $Z_{12}H_{12}^{2-}$ clusters, with X = {C, Si} and Z = {B, Al}.

[a] *Instituto de Química-Física Rocasolano (CSIC), Serrano 119, Madrid 28006, Spain*
[b] *Center for Computational Chemistry, University of Georgia, Athens, Georgia 30602, USA*
[c] *Departament de Química Inorgànica and Institut de Química Teòrica i Computacional (IQTCUB), Universitat de Barcelona, Diagonal 647, Barcelona 08028, Spain*
[d] *Instituto de Ciencias Matemáticas, CSIC-UAM-UCM-UC3M, Serrano 113, Madrid 28006, Spain*
[e] *Group of Complex Fluid Physics, Universidad de Almería, Almería 04120, Spain*
[f] *Instituto de Química Médica (CSIC), Juan de la Cierva 3, Madrid 28006, Spain*

† Presented at the XIV International Symposium on Small Particles and Inorganic Clusters, 15–19 September 2008, Valladolid, Spain.

‡ Electronic supplementary information (ESI) available: The experimental and computed symmetry-unique cage distances, Mulliken and natural bond orbital (NBO) charges, as well as the atom-in-molecules (AIM) topological analysis of the electron density for the $Z_{12}H_{12}^{2-}$ and r-$X_2Z_{10}H_{12}$ clusters; the continuous shape measures S_{IC} for the available crystal structures of the clusters included in this work (Table S3). See DOI: 10.1039/b924322d

2. Computational method

The computations were carried out with the program Gaussian03[28] and the B3LYP/6-311+G(d,p) model chemistry, which corresponds to a hybrid functional derived from density functional and Hartree–Fock theory.[28] The basis set is of triple-ζ type and includes one set of polarization functions for all atoms and one set of diffuse functions for all non-hydrogen atoms. All geometries presented in this work correspond to energy minima which were checked through analytical vibrational analysis.

With regards to polyhedral distortion in the clusters, continuous shape measures have been carried out using the Shape program,[29] in which Z_{12} and X_2Z_{10} cores have been considered as polyhedra.

3. Results and discussion

3.1 Molecular geometries

***r*-Carboranes/*r*-$C_2B_{10}H_{12}$.** The optimized geometries of compounds $Z_{12}H_{12}^{2-}$ and *r*-$X_2Z_{10}H_{12}$, X = {C, Si} and Z = {B, Al}, are displayed in Fig. 1, where only symmetry-unique X_i–X_j, X_i–Z_j and Z_i–Z_j distances are displayed. With regards to the $B_{12}H_{12}^{2-}$, $Al_{12}H_{12}^{2-}$, *r*-$C_2B_{10}H_{12}$ and *r*-$Si_2B_{10}H_{12}$ clusters (Fig. 1), the optimized geometries compare very well with the X-ray structures—where available—with a maximum relative error $<1\%$ (see ESI‡). In icosahedral *r*-$C_2B_{10}H_{12}$ carboranes, the fluxional character of the carbon atoms around the cage is well known,[30–32] with transitions *ortho* → *meta* at 600 °C and *meta* → *para* at 700 °C. The C–C distance in *o*-$C_2B_{10}H_{12}$ (Fig. 2a)—R(CC) = 1.625 Å—corresponds to a "stretched" single C–C bond; previous computations at B3LYP/6-31G(d) and MP2/6-31G(d) level of theory in 1,2-doubly substituted *o*-carboranes[33] showed that the bond-critical point between the carbon atoms disappears approximately at R(CC) > 1.9 Å (*vide infra*). We should also emphasize that the experimental B–B distances in the radical anion $B_{12}H_{12}^{-\bullet}$ are very similar as compared to the dianion $B_{12}H_{12}^{2-}$,[34,35] hence showing the large electronic delocalization in the cage.

***r*-Silaboranes/*r*-$Si_2B_{10}H_{12}$.** Turning now to the *r*-silaboranes, previous computations on *o*-$Si_2B_{10}H_{12}$ are reported at the HF/6-31G(d) and B3LYP/6-31G(d) level of theory.[36] As for published X-ray structures, we compare the 1,2-Me_2-1,2-$Si_2B_{10}H_{12}$ silaborane[18] with the corresponding optimized geometry and a maximum relative error of 1.2% is found (see ESI‡), similar to *r*-carboranes. The experimental Si–Si distance in disilane H_3Si–SiH_3 is R(SiSi) = 2.320 Å,[37] and in *o*-$Si_2B_{10}H_{12}$ the computed distance is slightly shorter R(SiSi) = 2.314 Å, hence both are single Si–Si bonds. For the known compound 1,2-Me_2-1,2-$Si_2B_{10}H_{10}$, the experimental[18] and computed Si–Si distances (this work, see ESI‡) amount to 2.308 Å and 2.325 Å, respectively, with a relative error of 0.7%. With regards to silaboranes *m*-$Si_2B_{10}H_{12}$ and *p*-$Si_2B_{10}H_{12}$, no crystal structures with *exo* substitutions—no changes in the cage structure—were found in the literature.

***r*-Carbalanes/*r*-$C_2Al_{10}H_{12}$.** Several crystal structures with the icosahedral Al_{12} motif have been published.[21–24] However, no structures to our knowledge have been found regarding an *ortho*, *meta* or *para* distribution of carbon atoms in carbalane clusters *r*-$C_2Al_{10}H_{12}$. In Fig. 1 (h, i, j, k) the optimized geometries of the $Al_{12}H_{12}^{2-}$ and *r*-$C_2Al_{10}H_{12}$ alane and carbalane clusters are displayed respectively. For the $Al_{12}R_{12}^{2-}$ cluster, the experimental (R = THF and R = $AlCl_2THF$) and computed (R = H) Al–Al distances compare very well (error ∼ 0.1%). As for the *r*-$C_2Al_{10}H_{12}$ structures, the distortion of the cage is noticeable due to smaller atom size for carbon atoms. The degree of distortion of the cages will be discussed further below in another section of this work. As depicted in Fig. 2i, the C–C distance in the *o*-$C_2Al_{10}H_{12}$ compound—1.632 Å—is not that far from the same distance in the carborane analogue *o*-$C_2B_{10}H_{12}$—1.625 Å. A topological analysis of the electron density shows that the electron density, ρ, in the bond critical point located in the middle of the C–C distance amounts to 1.246 *e* Å^{-3} and 1.243 *e* Å^{-3} for *o*-$C_2B_{10}H_{12}$ and *o*-$C_2Al_{10}H_{12}$, respectively, and therefore we can consider in both cases the presence of a stretched single C–C bond in both clusters. Note, however, the different electronic structure in the neighborhood around both carbon atoms in *o*-$C_2B_{10}H_{12}$ and *o*-$C_2Al_{10}H_{12}$.

***r*-Silalanes/*r*-$Si_2Al_{10}H_{12}$.** Finally, the optimized geometries of the silalane clusters, *r*-$Si_2Al_{10}H_{12}$, are depicted in Fig. 1 (l, m, n). Since the cage atoms belong to the same row of the periodic table, the cage distortions are similar to those found in the *r*-carborane analogues. The Si–Si bond distance in *o*-$Si_2Al_{10}H_{12}$—R(Si–Si) = 2.448 Å—is slightly longer as compared to the bond distance in disilane H_3Si–SiH_3, R(Si–Si) = 2.320 Å[37] due to electronic effects, as in *o*-$C_2B_{10}H_{12}$, and to the fact that the icosahedral cage is a supported structure. Therefore, we can conclude that we have a slightly stretched single Si–Si bond in *o*-$Si_2Al_{10}H_{12}$.

3.2 Electronic structure

Turning now to the stability factors in these clusters, Fig. 2 depicts the HOMO–LUMO gaps (E_g) which lie within a 4–9 eV energy window. The most stable clusters correspond to the well known carboranes (X = C, Y = B)—top of Fig. 2—with $E_g \approx 8$ eV. The least stable clusters correspond to 12-vertex carbalanes and silalanes, *r*-$X_2Al_{10}H_{12}$, X = {C, Si}, hence the difficulty in their experimental detection—note the almost degenerate energy gaps, E_g, for these clusters in Fig. 2 and similar indeed to the E_g for alane $Al_{12}H_{12}^{2-}$. Within given X and Y, the stability follows: *para* > *meta* > *ortho*, except for carbalane *r*-$C_2Al_{10}H_{12}$ where $E_g(ortho) \approx E_g(meta) \geq E_g(para)$.

3.2.1 Population analysis. Since NPA and Mulliken analysis show similar trends, only the former (NPA) will be discussed in this work due to their more realistic values (Table S2 in the ESI‡). In an attempt to estimate the changes introduced by the substitution of two X atoms by two Z atoms in the $Z_{12}H_{12}^{2-}$ cages in *ortho*, *meta* or *para* positions, we explore the atomic charges in homoatomic cages and then we turn to the heteroatomic cages. The NPA

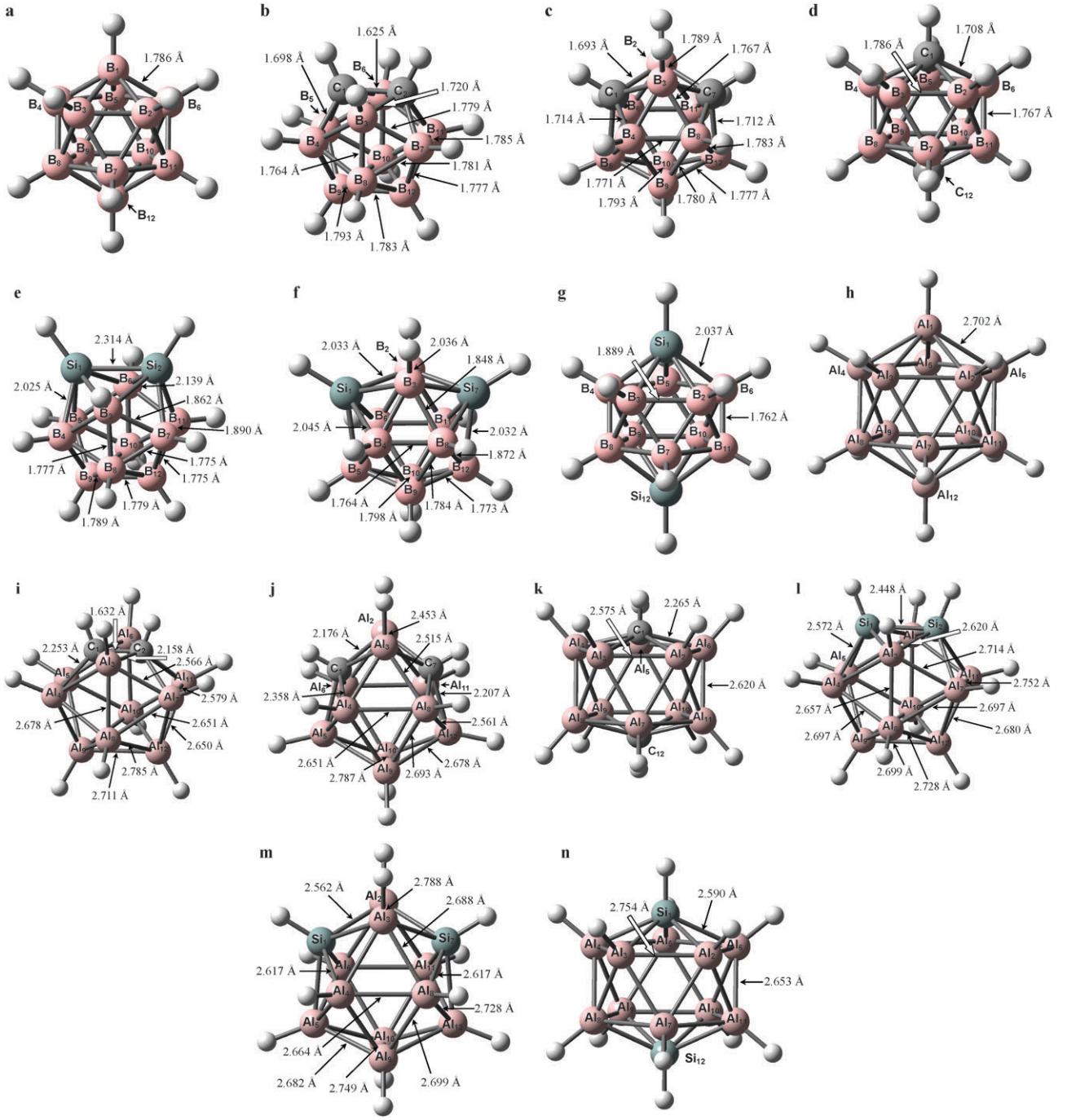

Fig. 1 Optimized geometries of the $Z_{12}H_{12}^{2-}$ and *r*-$X_2Z_{10}H_{12}$ clusters included in this work, *r* = {*ortho*, *meta*, *para*}, X = {C, Si}, Z = {B, Al}. Computations were performed with the B3LYP/6-311+G(d,p) model chemistry. Only symmetry-unique atom-atom distances are shown. A solid line connecting two atoms does not necessarily mean a chemical bond.

charges—Table 1—show a major population of valence orbitals for B rather than Al in $Z_{12}H_{12}^{2-}$ cages, represented by a more negative charge (−0.18 and +0.12, respectively). These results can be easily rationalized as a function of higher electronegativity from B to Al. As must be expected, the H atoms show inverse variation when both cages are compared (Table S2 in the ESI‡).

We now turn to the charges in heteroatomic cages. In general, when a highly electronegative X atom replaces a Z atom in a $Z_{12}H_{12}^{2-}$ cluster, such as in $XZ_{11}H_{12}^{-}$ or *r*-$X_2Z_{10}H_{12}$ cages, one can expect that electron density moves towards X, resulting in a more negative charge for this atom. This trend is clearly observed for *r*-$C_2Z_{10}H_{12}$ (Z = B, Al) and *r*-$Si_2Al_{10}H_{12}$ compounds, but an inverse effect is obtained in *r*-$Si_2B_{10}H_{12}$ as anticipated by comparison of electronegativities in Si and B (1.90 and 2.04, respectively).

A more detailed analysis of the population analysis reveals that the electron reorganization can be associated with

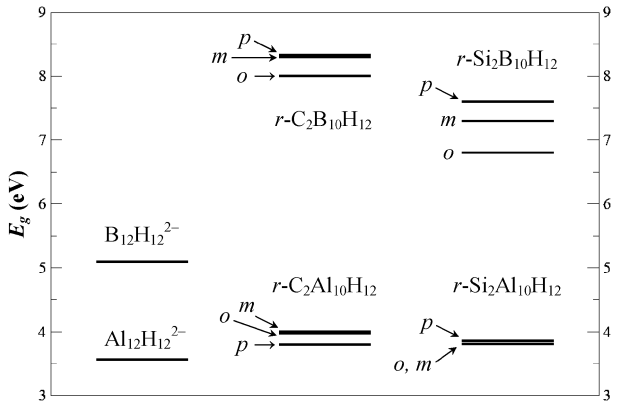

Fig. 2 Energy gaps, E_g, for the $Z_{12}H_{12}^{2-}$ and r-$X_2Z_{10}H_{12}$ clusters included in this work, r = {*ortho*, *meta*, *para*}, X = {C, Si}, Z = {B, Al}. Computations were performed with the B3LYP/6-311+G(d,p) model chemistry.

Table 1 Cage atoms X and Z natural population analysis (NPA) charges (in units of $|e|$) for the $Z_{12}H_{12}^{2-}$ and r-$X_2Z_{10}H_{12}$ clusters included in this work. Computations on the optimized geometries at B3LYP/6-311+G(d,p) level of theory. Note: the atom labels follow from Fig. 1

Cluster	Atom	q(NPA)	Cluster	Atom	q(NPA)
$B_{12}H_{12}^{2-}$	B_1	−0.175	—	—	—
$Al_{12}H_{12}^{2-}$	Al_1	0.117	—	—	—
o-$C_2B_{10}H_{12}$	C_1	−0.496	*o*-$Si_2B_{10}H_{12}$	Si_1	0.892
	B_3	0.158	—	B_3	−0.333
	B_4	0.000	—	B_4	−0.286
	B_8	−0.165	—	B_8	−0.185
	B_9	−0.139	—	B_9	−0.153
m-$C_2B_{10}H_{12}$	C_1	−0.639	*m*-$Si_2B_{10}H_{12}$	Si_1	1.083
	B_3	0.149	—	B_3	−0.436
	B_4	−0.021	—	B_4	−0.280
	B_5	0.058	—	B_5	−0.267
	B_9	−0.176	—	B_9	−0.173
p-$C_2B_{10}H_{12}$	C_1	−0.664	*p*-$Si_2B_{10}H_{12}$	Si_1	1.094
	B_2	0.005	—	B_2	−0.289
Cluster	Atom	q(NBO)	Cluster	Atom	q(NBO)
o-$C_2Al_{10}H_{12}$	C_1	−1.239	*o*-$Si_2Al_{10}H_{12}$	Si_1	−0.196
	Al_3	0.805	—	Al_3	0.392
	Al_4	0.442	—	Al_4	0.294
	Al_8	0.240	—	Al_8	0.186
	Al_9	0.239	—	Al_9	0.201
m-$C_2Al_{10}H_{12}$	C_1	−1.623	*m*-$Si_2Al_{10}H_{12}$	Si_1	−0.320
	Al_3	0.819	—	Al_3	0.408
	Al_4	0.503	—	Al_4	0.296
	Al_5	0.505	—	Al_5	0.313
	Al_9	0.208	—	Al_9	0.176
p-$C_2Al_{10}H_{12}$	C_1	−1.604	*p*-$Si_2Al_{10}H_{12}$	Si_1	−0.324
	Al_2	0.500	—	Al_2	0.299

electronegativity differences $\chi(Z)-\chi(X)$ and q_X charges in X atoms, which follow as: $C_2Al_{10} < C_2B_{10} < Si_2Al_{10} < Si_2B_{10}$. With regards to the relative positions of the two X atoms—*ortho*, *meta*, or *para*—similar charges are obtained for *meta* and *para* isomers with a range of 2.7 electrons (−1.6, −0.7, 0.3, and 1.1, respectively), but this decreases to 2.1 electrons in the *ortho* derivative (−1.2, −0.5, −0.2, and 0.9, respectively). This dramatic change can be related to the presence of an X–X bond in the *ortho*-$X_2Z_{10}H_{12}$ cages, and the chemical properties of this bonding, such as electron-precise and localized nature (see *Topological analysis* below). In addition, the charges in X-bound hydrogens have similar values in all cases and only depend on X.

The analysis of the charges in Z atoms is very simple for *para*-$X_2Z_{10}H_{12}$ cages where ten Z atoms are equivalent by symmetry. In this case, Z-charges, q_Z, follow the order $C_2Al_{10} > Si_2Al_{10} > C_2B_{10} > Si_2B_{10}$ due to the electronegativity of Z with small range for Z than that obtained for X atoms. These differences can be understood as a compensation of the changes introduced by X in an ideal $Z_{12}H_{12}^{2-}$ cage. However, *ortho* and *meta* clusters involve a more complicated analysis due to the non-equivalent positions; however, a general tendency is observed where Z atoms near X have positive charge (low electron population in Z) when X is more electronegative than Z, as in C_2B_{10}, C_2Al_{10}, and Si_2Al_{10}, whereas negative charge is found in r-$Si_2B_{10}H_{12}$ due to this inverse order. Finally, small changes in hydrogen charges in H(Z) are observed and depend only on the position in the isomeric forms, mainly determined only by the Z atom.

3.2.2 Topological analysis of the electron density in r-$X_2Z_{10}H_{12}$ and $Z_{12}H_{12}^{2-}$ clusters. The topological analysis of the electron density provides a large variety of motifs in the systems studied. In all cases, the Poincaré-Hopf relationship which relates the number of critical points present in a given system is fulfilled. Only five of the molecules studied ($B_{12}H_{12}^{2-}$, $Al_{12}H_{12}^{2-}$, *o*-$C_2B_{10}H_{12}$, *o*-$Si_2Al_{10}H_{12}$ and *m*-$Si_2B_{10}H_{12}$) show the expected bond pattern (42: 30 between the cage atoms and 12 between cage and hydrogen atoms) and the corresponding rings and cages (20 and 1, respectively). In seven cases, fewer bonds than expected are found while in two cases, we find more than 42 bonds. In all cases, these discrepancies are due to the cage atoms only (see the molecular graphs in the ESI‡).

Among those cases with fewer bonds, four patterns are found: (*i*) the cluster *o*-$Si_2B_{10}H_{12}$, where the bonds between the silicon atoms and the borons in position 3 and 6 are missing, as well as those between B_4–B_5 and the symmetrical B_7–B_{11} (for the labels assigned to cage atoms, see Fig. 1); (*ii*) the carbalane *m*-$C_2Al_{10}H_{12}$ shows a long C···C bonding interaction (3.02 Å) while no bond or bonding interactions are found between the carbon atoms and Al_2 and Al_3; (*iii*) the clusters *m*-$C_2B_{10}H_{12}$ and *m*-$Si_2Al_{10}H_{12}$ lack the Z_2–Z_3 bond; and finally (*iv*) in clusters *p*-$C_2B_{10}H_{12}$, *p*-$Si_2B_{10}H_{12}$, and *p*-$Si_2Al_{10}H_{12}$, no bond-critical point (bcp) is detected between Z_2 and Z_3 and the corresponding equivalent connections (Z_3–Z_4, Z_4–Z_5, Z_5–Z_6, Z_2–Z_6, Z_7–Z_8, Z_8–Z_9, Z_9–Z_{10}, Z_{10}–Z_{11} and Z_7–Z_{11}, see Fig. 1 and the ESI‡).

As shown in Table 2, the two cases with more than 42 bonds correspond to clusters *o*-$C_2Al_{10}H_{12}$ and *p*-$C_2Al_{10}H_{12}$, where the carbon atoms are involved in several independent bonds with the same aluminium atom. In addition, in *p*-$C_2Al_{10}H_{12}$ a C···C bonding interaction appears along the C_5 rotation axis with an intermolecular distance of 3.40 Å. However, this bond-critical point (bcp) is surrounded by five ring critical points (rcp) and cage critical points (ccp) in close proximity, an indication of the possibility of a near catastrophic description of the electron density. A small elongation of the C···C distance will collapse all these critical points onto a single ccp. The *p*-$C_2Al_{10}H_{12}$ molecule presents 12 bcp's associated to each of the carbon atoms.

Table 2 Critical points computed for the $Z_{12}H_{12}^{2-}$ and *r*-$X_2Z_{10}H_{12}$ clusters included in this work (B3LYP/6-311+G(d,p) model chemistry computations); "bcp", "rcp" and "ccp" stand for bond, ring and cage critical point, respectively

	bcp's	rcp's	ccp's
$Al_{12}H_{12}^{2-}$	42	20	1
$B_{12}H_{12}^{2-}$	42	20	1
o-$C_2Al_{10}H_{12}$	48	26	1
o-$C_2B_{10}H_{12}$	42	20	1
o-$Si_2Al_{10}H_{12}$	42	20	1
o-$Si_2B_{10}H_{12}$	36	14	1
m-$C_2Al_{10}H_{12}$	40	18	1
m-$C_2B_{10}H_{12}$	41	19	1
m-$Si_2Al_{10}H_{12}$	41	19	1
m-$Si_2B_{10}H_{12}$	42	20	1
p-$C_2Al_{10}H_{12}$	53	35	5
p-$C_2B_{10}H_{12}$	32	10	1
p-$Si_2Al_{10}H_{12}$	32	10	1
p-$Si_2B_{10}H_{12}$	32	10	1

In order to analyze the nature of the bonding associated to each bcp, we have used the values of the electron density, ρ, and the total energy density, H, at this point. The latter parameter has been shown to be more efficient in order to elucidate the covalent or ionic nature of the interactions. In Table 3 we gather the range of values computed for these two parameters in the unique bcp's. In all cases, negative values of H are obtained, with the exception of one of the long C···C bonding interactions that shows a positive sign in this parameter. Thus, the bonds between the heavy atoms can be considered as covalent. In general, shorter bonds of each type are associated with larger values and more negative values of H, which is the opposite for longer bonds.

3.3 Polyhedral distortion in *r*-$X_2Z_{10}H_{12}$ and $Z_{12}H_{12}^{2-}$ clusters

3.3.1 Volumes, skewness, and kurtosis. Table 4 collects the polyhedral volumes of the perfect and distorted icosahedral cages for the $Z_{12}H_{12}^{2-}$ and r-$X_2Z_{10}H_{12}$ clusters, taking the cage nuclei as dimensionless points in an (distorted) icosahedral polyhedron. The volume of a polyhedron is a first order parameter for evaluating the degree of distortion. Table 4 shows that substitution of two B atoms in the cage of $B_{12}H_{12}^{2-}$ by two C atoms (and leading to neutral species *r*-$C_2B_{10}H_{12}$) in *ortho*, *meta* or *para* positions implies a contraction of 5.2%, 5.8% and 5.9% of the cage volume, respectively. A cage contraction also occurs for the $Al_{12}H_{12}^{2-}$ cluster when two Al atoms are substituted by two Si atoms in *ortho*, *meta* or *para* positions, leading to cage volume contractions of 4.3%, 4.7% and 5.0%, respectively, similar to the case for atoms one row above in the periodic table. When crossing columns of the periodic table in different rows, the icosahedral cages logically distort to a greater extent due to atom size differences; hence larger cage volume contractions and expansions take place for the transitions: $Al_{12}H_{12}^{2-}$ → *r*-$C_2Al_{10}H_{12}$, with 22.6%, 24.0% and 25.6% contraction for *ortho*, *meta* an *para* isomers, respectively; $B_{12}H_{12}^{2-}$ → *r*-$Si_2B_{10}H_{12}$, with 19.3%, 18.7%, and 18.7% expansion for *ortho*, *meta* an *para* isomers, respectively.

Table 4 Cage polyhedral volumes (in Å^3) of clusters $Z_{12}H_{12}^{2-}$ and *r*-$X_2Z_{10}H_{12}$, Z = B, Al, X = Si, *r* = *ortho*, *meta*, *para* with B3LYP/6-311+G(d,p) model chemistry computations. All cage geometries correspond to energy minima. For the computation of the cage volumes, we take as polyhedral vertices the nuclei positions of atoms X and Z in the (distorted) icosahedral cage and sum over all twenty tetrahedra (see ref. 38). The distortion index is defined as $i_d = V(r\text{-}X_2Z_{10}H_{12})/V(Z_{12}H_{12}^{2-}) - 1 \times 100$, and can be positive for an expansion or negative for a contraction

	X	Z	V	i_d
$Z_{12}H_{12}^{2-}$	—	B	12.44	0.0
$Z_{12}H_{12}^{2-}$	—	Al	43.04	0.0
o-$X_2Z_{10}H_{12}$	C	B	11.79	−5.23
	Si	B	14.84	+19.29
m-$X_2Z_{10}H_{12}$	C	B	11.72	−5.79
	Si	B	14.77	+18.73
p-$X_2Z_{10}H_{12}$	C	B	11.71	−5.87
	Si	B	14.76	+18.65
o-$X_2Z_{10}H_{12}$	C	Al	33.32	−22.58
	Si	Al	41.19	−4.30
m-$X_2Z_{10}H_{12}$	C	Al	32.99	−23.99
	Si	Al	41.01	−4.72
p-$X_2Z_{10}H_{12}$	C	Al	32.01	−25.63
	Si	Al	40.91	−4.95

In order to study the distortion of the clusters to a major extent, we make use of the covariance matrix. In the *ortho* and *meta* cases, we compute the skewness of the cluster and in the *para* case, we compute the kurtosis of the cluster.

Given a cluster of points $\{(x_i, y_i, z_i)\}$, $i = 1,\ldots,M$ such that

$$\sum_{i=1}^{M} x_i = \sum_{i=1}^{M} y_i = \sum_{i=1}^{M} z_i = 0, \qquad (1)$$

Table 3 Range of interatomic distances, electron density, ρ, and total energy density, H, in the bond critical points of $X_{12}H_{12}^{2-}$ and *r*-$X_2Z_{10}H_{12}$ clusters (B3LYP/6-311+G(d,p) model chemistry computations)

	Dist./Å		ρ/e Å^{-3}		H/Hartree Å^{-3}		
Atom–Atom	Min.	Max.	Max.	Min.	Max.	Min.	Number of bonds[a]
B–B	1.762	2.036	0.830	0.567	−0.216	−0.513	25
Al–Al	2.515	2.787	0.324	0.250	−0.067	−0.135	23
B–C	1.693	1.720	0.871	0.796	−0.628	−0.742	6
B–Si	2.025	2.045	0.641	0.628	−0.412	−0.432	5
Al–C	2.158	2.358	0.364	0.277	−0.067	−0.115	8
Al–Si	2.562	2.620	0.310	0.277	−0.101	−0.121	6
C–C	1.625	3.400	1.248	0.054	0.007	−0.803	4

[a] In certain cases, we refer to "bond" as a "bonding interaction"—*e.g.* a C···C distance of 3.4 Å in *p*-$C_2Al_{10}H_{12}$—last row.

the covariance matrix is the 3 by 3 symmetric matrix C, with entries

$$\frac{1}{M}C_{xx} = \sum_{i=1}^{M} x_i^2,\ \frac{1}{M}C_{yy} = \sum_{i=1}^{M} y_i^2,\ \frac{1}{M}C_{zz} = \sum_{i=1}^{M} z_i^2,$$
$$\frac{1}{M}C_{xy} = \sum_{i=1}^{M} x_i y_i,\ \frac{1}{M}C_{xz} = \sum_{i=1}^{M} x_i z_i,\ \frac{1}{M}C_{yz} = \sum_{i=1}^{M} y_i z_i. \quad (2)$$

The eigenvectors of this matrix are the principal axes and the square root of its eigenvalues measure the dispersion of the cluster in each direction. The square roots of the eigenvalues are called the semiaxis. Given the symmetries of the clusters we are studying, we know *a priori* the principal axes. In the case of $Z_{12}H_{12}^{2-}$, any axis is a principal axis and all the eigenvalues have the same value. In the case of *p*-$X_2Z_{10}H_{12}$, a principal axis joins the center with one of the X atoms. By convention, we take this as the z axis. Any orthogonal vector will also be a principal axis. In this case, two semiaxes will have the same value. In the cases of *o*-$X_2Z_{10}H_{12}$ and *m*-$X_2Z_{10}H_{12}$, one principal axis joins the center with the middle point of the segment between the two X atoms. By convention, we will take this as the z axis with the X atoms with negative z coordinates. The second principal axis lies in the plane containing the center and the two X atoms and is orthogonal to the previous one. By convention, we will take this as the y axis. The third principal axis is orthogonal to the previous two. In these cases, all the semiaxes may be different. We will denote the semiaxes by s_x, s_y and s_z.

In order to measure the distortion of the cluster of points, we compute the differences between the semiaxes divided by s_x:

$$\delta_{zx} = \frac{s_z - s_x}{s_x}, \delta_{yx} = \frac{s_y - s_x}{s_x}, \delta_{zy} = \frac{s_z - s_y}{s_x}. \quad (3)$$

We only compute the distortions that are relevant to each geometry. Once we have chosen coordinates as before, the skewness (along the z axis) is given by

$$\gamma_1 = \frac{\frac{1}{M}\sum_{i=1}^{M} z_i^3}{\left(\frac{1}{M}\sum_{i=1}^{M} z_i^2\right)^{3/2}} \quad (4)$$

The skewness measures the asymmetry of the distribution of points on both sides of the center. In the cases of $Z_{12}H_{12}^{2-}$ and *p*-$X_2Z_{10}H_{12}$, the skewness is zero. In the cases of *o*-$X_2Z_{10}H_{12}$ and *m*-$X_2Z_{10}H_{12}$, only the skewness along the z axis may be non zero.

The kurtosis (along the z axis) is given by

$$k_z = \frac{\frac{1}{M}\sum_{i=1}^{M} z_i^4}{\left(\frac{1}{M}\sum_{i=1}^{M} z_i^2\right)^{2}} \quad (5)$$

The kurtosis measures the peakedness of the distribution of points on both sides of the center. In the icosahedral case, the kurtosis is 1.8.

Table 5 Semiaxes and kurtosis for icosahedral cages $Z_{12}H_{12}^{2-}$, Z = {B, Al}

Cluster	s_x cage	k_z cage	s_x hydrogen	k_z hydrogen
$B_{12}H_{12}^{2-}$	0.981	1.8	1.675	1.8
$Al_{12}H_{12}^{2-}$	1.484	1.8	2.411	1.8

In Table 5–8 we report the semiaxes, the distortion, the skewness (in the *ortho* and *meta* cases) and the kurtosis (in the *para* case) of the different clusters. For each cluster, we compute these values separately for the cage atoms only (entry "cage") and for hydrogen atoms only (entry "hydrogen").

In the *para* clusters, we observe that in one case the distortion of the cage is negligible (less than 1%), while in the other three cases the distortion is negative. This means that the z axis is shorter than the other two axes. By contrast, the distortion of the distribution of hydrogen atoms is always positive, *i.e.* the z axis is longer that the other two. A similar phenomenon is observed in the *ortho* and *meta* cases: the distortions δ_{zx} and δ_{yx} of the cage are negative for three of the compounds, while they are all positive for the distribution of hydrogen atoms. In all the cases, the biggest distortion is obtained for $C_2Al_{10}H_{12}$.

We also observe that in all cases the skewness of the distribution of hydrogen atoms is always smaller (*i.e.* more negative) that the skewness of the cage. That is, the distribution of hydrogen atoms is more distorted than the inner cage.

If the kurtosis is small/large (compared to 1.8, the icosahedral case) the apical atoms are flattened/stretched along the z axis—see Fig. 1. There are two facts that explain the kurtosis: the size of the atom and the charge of the hydrogen atoms. One extreme case is *p*-$C_2Al_{10}H_{12}$, where the carbon atoms are smaller than the aluminium atoms and the repulsion between the negatively charged hydrogen atoms results in an almost cylindrical shape. At the other extreme lies the *p*-$Si_2B_{10}H_{12}$, where the size of the atoms and distribution of charges result in the silicon atoms being stretched along the z axis, with corresponding larger kurtosis. In all cases, the kurtosis of the cage is always closer to the icosahedral value (1.8) than the kurtosis of the hydrogen atoms.

3.3.2 Continuous shape measures. An alternative way to summarize changes in structural parameters consists of using the continuous shape measures, which provide quantitative information of how much the environment deviates from an ideal polyhedron. In brief, a zero value of the icosahedral shape measure (S_{IC}, or icosahedricity) indicates that the structure of the polyhedron, X_2Z_{10}, under scrutiny has exactly the shape of the ideal icosahedron, and it increases as any structural parameter is distorted. As a rule of thumb, values smaller than 0.1 correspond to minute deviations from the ideal shape, while a value of one unit or larger indicates an important distortion.[39]

The S_{IC} computed values for *r*-$X_2Z_{10}H_{12}$ and $Z_{12}H_{12}^{2-}$ clusters are shown in Table 9 (S_{IC} values for known crystal structures are available in the ESI‡). As expected, homonuclear cages such as $B_{12}H_{12}^{2-}$ and $Al_{12}H_{12}^{2-}$ have the perfect I_h symmetry of an icosahedron, in agreement with the

Table 6 Semiaxes and distortion in the "*para*" clusters

Cluster	s_x cage	δ_{zx} cage	k_z cage	s_x hydrogen	δ_{zx} hydrogen	k_z hydrogen
p-$C_2B_{10}H_{12}$	0.980	−0.057	1.60	1.625	0.012	1.46
p-$Si_2B_{10}H_{12}$	1.037	0.008	2.33	1.723	0.052	2.37
p-$C_2Al_{10}H_{12}$	1.414	−0.125	1.16	2.110	0.122	1.03
p-$Si_2Al_{10}H_{12}$	1.512	−0.100	1.55	2.327	0.036	1.37

Table 7 Semiaxes, distortion and skewness of the clusters in the "*ortho*" and "*meta*" cases, without hydrogen atoms

Cluster	s_x	δ_{zx}	δ_{yx}	δ_{zy}	γ_1
o-$C_2B_{10}H_{12}$	0.986	−0.045	−0.019	−0.025	0.237
o-$Si_2B_{10}H_{12}$	1.037	0.060	0.003	0.057	0.680
o-$C_2Al_{10}H_{12}$	1.442	−0.096	−0.057	−0.039	0.028
o-$Si_2Al_{10}H_{12}$	1.513	−0.070	−0.028	−0.042	0.152
m-$C_2B_{10}H_{12}$	0.982	−0.018	−0.042	0.023	0.100
m-$Si_2B_{10}H_{12}$	1.041	0.015	0.004	0.011	0.526
m-$C_2Al_{10}H_{12}$	1.454	−0.071	−0.114	0.043	−0.065
m-$Si_2Al_{10}H_{12}$	1.515	−0.034	−0.072	0.038	0.040

Table 8 Semiaxes, distortion and skewness of the clusters in the "*ortho*" and "*meta*" cases, without the cage atoms (hydrogen atoms only)

Cluster	s_x	δ_{zx}	δ_{yx}	δ_{zy}	γ_1
o-$C_2B_{10}H_{12}$	1.630	0.004	0.003	0.001	0.093
o-$Si_2B_{10}H_{12}$	1.726	0.044	0.020	0.024	0.307
o-$C_2Al_{10}H_{12}$	2.134	0.080	0.036	0.044	−0.043
o-$Si_2Al_{10}H_{12}$	2.333	0.022	0.009	0.013	0.001
m-$C_2B_{10}H_{12}$	1.624	0.005	0.010	−0.005	0.003
m-$Si_2B_{10}H_{12}$	1.728	0.016	0.033	−0.017	0.290
m-$C_2Al_{10}H_{12}$	2.124	0.056	0.074	−0.018	−0.159
m-$Si_2Al_{10}H_{12}$	2.321	0.019	0.028	−0.009	−0.062

experimental value (<0.06 and 0.03, respectively). When two atoms of Z are replaced by X in a X_2Z_{10} cage, less distorted structures are always found for the C_2B_{10} cages, probably due to the similar size of boron and carbon atoms, and also less diffuse orbitals (experimental values are always less than 0.30). Moreover, the largest values of S_{IC} are obtained in the C_2Al_{10} polyhedron, indicating that the steric and electronic requirements of carbon atoms in an aluminium polyhedron must be inappropriate. As should be expected, intermediate values are found in silicon cages, for which only experimental structures of *ortho*-Si_2B_{10} compounds have been reported so far, and which have structurally similar values to the computed one (~0.6).

Finally, the values of S_{IC} for heteronuclear cages are less influenced by the isomeric form. Given the C_2B_{10} and Si_2Al_{10} cages, where atoms within a cluster have similar sizes, the *ortho* isomer is always the most symmetric one and there is an inversion of the degree of distortion between the *para* and *meta* isomers. Interestingly, for a X_2Z_{10} cage, changing the row of the periodic table for Z results in a complete inversion of the degree of distortion, independently from the X atom.

Table 9 Icosahedral shape measure (S_{IC}) for polyhedra X_2Z_{10} and Z_{12}

	S_{IC}			
Formula	*ortho*	*meta*	*para*	$Z_{12}H_{12}^{2-}$
r-$C_2B_{10}H_{12}$	0.116	0.181	0.143	0.000
r-$Si_2B_{10}H_{12}$	0.582	0.365	0.321	
r-$C_2Al_{10}H_{12}$	1.902	1.251	1.462	0.000
r-$Si_2Al_{10}H_{12}$	0.186	0.200	0.340	

4. Conclusions

We have shown how the electronic structures and geometries of the clusters $Z_{12}H_{12}^{2-}$ and *r*-$X_2Z_{10}H_{12}$ vary as a function of atoms X = {C, Si} and Z = {B, Al}. As for the well known borane $B_{12}H_{12}^{2-}$ and carboranes *r*-$C_2B_{10}H_{12}$, their well known exploited chemistries arise from the large HOMO–LUMO gap (~8 eV), which also explains their stability; substitution of carbon by silicon in *r*-$C_2B_{10}H_{12}$ decreases the stability by ~1 eV. Clusters derived from alane $Al_{12}H_{12}^{2-}$ with substitution of two C and Si atoms in the cage have similar reactivities as the alane itself, given the HOMO–LUMO gaps (~3.5 eV).

The topological analysis of the density in these clusters also indicates very different electronic structures, especially surrounding the regions of the X atoms when changing the row of the periodic table as compared to the main cage atoms, Z. Continuous shape measures show that only the *r*-C_2Al_{10} cluster involves large deviations from the perfect icosahedron.

Important future goals within this research project include the study of the *r*-$X_2Z_{10}H_{12}$ and $Z_{12}H_{12}^{2-}$ type of clusters as a function of charge, spin multiplicity, excited state nature and properties of architectures derived therein from their assembly in different dimensions, in a similar fashion as we have described the related research line in a recent publication for *r*-carborane chemistry.[26]

Acknowledgements

This work was funded by projects CTQ2008-06670-C02-01/BQU (GA) and MAT2009-14234-C03-02 (JMO). We are indebted to Dr Alexander Goldberg (Accelrys, San Diego) for helpful discussions.

References

1 H. Jude, H. Disteldorf, S. Fischer, T. Wedge, A. M. Hawkridge, A. M. Arif, M. F. Hawthorne, D. C. Muddiman and P. J. Stang, *J. Am. Chem. Soc.*, 2005, **127**, 12131.
2 See "Recent Advances in Boron Chemistry", *Journal of Organometallic Chemistry*, ed. F. Teixidor, 2009, vol. 694.
3 R. C. Reynolds, S. R. Campbell, R. G. Fairchild, R. L. Kisliuk, P. L. Micca, S. F. Queener, J. M. Riordan, W. D. Sedwick, W. R. Waud, A. K. W. Leung, R. W. Dixon, W. J. Suling and D. W. Borhani, *J. Med. Chem.*, 2007, **50**, 3283.
4 N. Zine, J. Bausells, A. Ivorra, J. Aguilo, M. Zabala, F. Teixidor, C. Masalles, C. Vinas and A. Errachid, *Sens. Actuators, B*, 2003, **91**, 76.

5 B. Grüner, J. Plesek, J. Baca, I. Cisarova, J.-F. Dozol, H. Roquette, C. Viñas, P. Selucky and J. Rais, *New J. Chem.*, 2002, **26**, 1519.
6 O. I. Buzhinsky, V. G. Ostroshchenko, D. G. Whyte, M. Baldwin, R. W. Conn, R. P. Doerner, R. Seraydarian, S. Luckhardt, H. Kugel and W. P. West, *J. Nucl. Mater.*, 2003, **313–316**, 214.
7 D. Tafalla and F. L. Tabares, *Vacuum*, 2002, **67**, 393.
8 R. Hamasaki, M. Ito, M. Lamrani, M. Mitsuishi, T. Myashita and Y. Yamamoto, *J. Mater. Chem.*, 2003, **13**, 21.
9 H. Shen, H. S. Chan and Z. W. Xie, *Organometallics*, 2008, **27**, 5309.
10 P. J. Collings, *Liquid Crystals*, Princeton Univ. Press, Princeton, NJ, 2nd edn, 2001.
11 M. Ito, F. Nakamura, A. Baba, K. Tamada, H. Ushijima, K. Hang, A. Lau, A. Manna and W. Knoll, *J. Phys. Chem. C*, 2007, **111**, 11653.
12 K. Kokado and Y. Chujo, *Macromolecules*, 2009, **42**, 1418.
13 S. A. Shackelford, J. L. Belletire, J. A. Boatz, S. Schneider, A. K. Wheaton, B. A. Wight, L. M. Hudgens, H. L. Ammon and S. H. Strauss, *Org. Lett.*, 2009, **11**, 2623.
14 M. F. Hawthorne, J. I. Zink, J. M. Skelton, M. J. Bayer, C. Liu, E. Livshits, R. Baer and D. Neuhauser, *Science*, 2004, **303**, 1849.
15 W. Jiang, D. E. Harwell, M. D. Mortimer, C. B. Knobler and M. F. Hawthorne, *Inorg. Chem.*, 1996, **35**, 4355.
16 J. Müller, K. Baše, T. F. Magnera and J. Michl, *J. Am. Chem. Soc.*, 1992, **114**, 9721.
17 H. Hiura and T. Kanayama, *J. Mol. Struct.*, 2005, **735–736**, 367.
18 D. Seyferth, K. Büchner, W. S. Rees Jr., and W. M. Davis, *Angew. Chem.*, 1990, **102**, 911; D. Seyferth, K. Büchner, W. S. Rees Jr., and W. M. Davis, *Angew. Chem., Int. Ed. Engl.*, 1990, **29**, 918.
19 L. Wesemann, Y. Ramjoie, M. Trinkaus and B. Ganter, *Z. Anorg. Allg. Chem.*, 1998, **624**, 1573.
20 L. Wesemann, M. Trinkaus, U. Englert and J. Muller, *Organometallics*, 1999, **18**, 4654.
21 C. Klemp, R. Koppe, E. Weckert and H. Schnockel, *Angew. Chem., Int. Ed.*, 1999, **38**, 1740.
22 K.-W. Klinkhammer, W. Uhl, J. Wagner and W. Hiller, *Angew. Chem., Int. Ed. Engl.*, 1991, **30**, 179.
23 C. Klemp, M. Bruns, J. Gauss, U. Haussermann, G. Stosser, L. van Wullen, M. Jansen and H. Schnockel, *J. Am. Chem. Soc.*, 2001, **123**, 9099.
24 J. Vollet, R. Burgert and H. Schnockel, *Angew. Chem., Int. Ed.*, 2005, **44**, 6956.
25 D. E. Bergeron, A. W. Castleman Jr., T. Morisato and S. N. Khanna, *Science*, 2004, **304**, 84.
26 J. M. Oliva, D. J. Klein, P. V. R. Schleyer and L. Serrano-Andrés, *Pure Appl. Chem.*, 2009, **81**, 719.
27 L. Serrano-Andrés and J. M. Oliva, *Chem. Phys. Lett.*, 2006, **432**, 235.
28 M. J. Frisch, G. W. Trucks, H. B. Schlegel, G. E. Scuseria, M. A. Robb, J. R. Cheeseman, J. A. Montgomery, Jr., T. Vreven, K. N. Kudin, J. C. Burant, J. M. Millam, S. S. Iyengar, J. Tomasi, V. Barone, B. Mennucci, M. Cossi, G. Scalmani, N. Rega, G. A. Petersson, H. Nakatsuji, M. Hada, M. Ehara, K. Toyota, R. Fukuda, J. Hasegawa, M. Ishida, T. Nakajima, Y. Honda, O. Kitao, H. Nakai, M. Klene, X. Li, J. E. Knox, H. P. Hratchian, J. B. Cross, V. Bakken, C. Adamo, J. Jaramillo, R. Gomperts, R. E. Stratmann, O. Yazyev, A. J. Austin, R. Cammi, C. Pomelli, J. Ochterski, P. Y. Ayala, K. Morokuma, G. A. Voth, P. Salvador, J. J. Dannenberg, V. G. Zakrzewski, S. Dapprich, A. D. Daniels, M. C. Strain, O. Farkas, D. K. Malick, A. D. Rabuck, K. Raghavachari, J. B. Foresman, J. V. Ortiz, Q. Cui, A. G. Baboul, S. Clifford, J. Cioslowski, B. B. Stefanov, G. Liu, A. Liashenko, P. Piskorz, I. Komaromi, R. L. Martin, D. J. Fox, T. Keith, M. A. Al-Laham, C. Y. Peng, A. Nanayakkara, M. Challacombe, P. M. W. Gill, B. G. Johnson, W. Chen, M. W. Wong, C. Gonzalez and J. A. Pople, *GAUSSIAN 03 (Revision C.02)*, Gaussian, Inc., Wallingford, CT, 2004.
29 M. Llunell, D. Casanova, J. Cirera, J. M. Bofill, P. Alemany and S. Alvarez, *Shape version 1.1a*, Universitat de Barcelona, Barcelona, Spain, 2003.
30 W. N. Lipscomb, *Science*, 1966, **153**, 373.
31 G. B. Dunks, R. J. Wiersma and M. F. Hawthorne, *J. Am. Chem. Soc.*, 1973, **95**, 3174.
32 K. Hermansson, M. Wójcik and S. Sjöberg, *Inorg. Chem.*, 1999, **38**, 6039.
33 J. M. Oliva, N. L. Allan, P. v. R. Schleyer, C. Viñas and F. Teixidor, *J. Am. Chem. Soc.*, 2005, **127**, 13538.
34 T. Peymann, C. B. Knobler and M. F. Hawthorne, *J. Am. Chem. Soc.*, 1999, **121**, 5601.
35 M. J. Ingleson, S. K. Brayshaw, M. F. Mahon, G. D. Ruggiero and A. S. Weller, *Inorg. Chem.*, 2005, **44**, 3162.
36 E. D. Jemmis and B. Kiran, *J. Am. Chem. Soc.*, 1997, **119**, 4076.
37 G. R. Gupte and R. Prasad, *Int. J. Mod. Phys. B*, 1998, **12**, 1607.
38 J. I. Burgos, L. Serrano-Andrés, J. M. Oliva and D. J. Klein, *Afinidad*, 2008, **533**, 32–38.
39 S. Alvarez, P. Alemany, D. Casanova, J. Cirera, M. Llunell and D. Avnir, *Coord. Chem. Rev.*, 2005, **249**, 1693.

